

1

2 *Supplement*

3

4 **Tropospheric aerosols over the western North Atlantic Ocean**
5 **during the winter and summer campaigns of ACTIVATE 2020:**
6 **Life cycle, transport, and distribution**

7

8 Hongyu Liu^{1,2}, Bo Zhang^{1,2}, Richard H. Moore², Luke D. Ziemba², Richard A. Ferrare², Hyundeok
9 Choi^{1,*}, Armin Sorooshian³, David Painemal^{2,4}, Hailong Wang⁵, Michael A. Shook², Amy Jo
10 Scarino^{2,4}, Johnathan W. Hair², Ewan C. Crosbie^{2,4}, Marta A. Fenn^{2,4}, Taylor J. Shingler², Chris A.
11 Hostetler², Gao Chen², Mary M. Kleb², Gan Luo⁶, Fangqun Yu⁶, Jason L. Tackett², Mark A.
12 Vaughan², Yongxiang Hu², Glenn S. Diskin², John B. Nowak², Joshua P. DiGangi², Yonghoon
13 Choi^{2,4}, Christoph A. Keller^{7,8}, and Matthew Johnson⁹

14 ¹National Institute of Aerospace, Hampton, VA

15 ²NASA Langley Research Center, Hampton, VA

16 ³University of Arizona, Tucson, AZ

17 ⁴Analytical Mechanics Associates, Hampton, VA

18 ⁵Pacific Northwest National Laboratory, Richland, WA

19 ⁶State University of New York at Albany, Albany, NY

20 ⁷Morgan State University, Baltimore, MD

21 ⁸NASA Goddard Space Flight Center, Greenbelt, MD

22 ⁹NASA Ames Research Center, Moffett Field, CA

23 ^{*}Now at SAIC / NOAA/NWS/NCEP/Environmental Modeling Center, College Park, MD

24

25 Correspondence to: Hongyu Liu (hongyu.liu-1@nasa.gov); Bo Zhang (bo.zhang@nasa.gov)

26

27 **Section S1: Model evaluation with surface aerosol concentrations, deposition fluxes, and MODIS AOD**

28

28 **observations**

29 In this section we evaluate model simulations with surface aerosol concentration observations from the
30 IMPROVE and CSN networks, aerosol deposition flux measurements from the NTN network of NADP, and satellite
31 AOD measurements from MODIS/Aqua, with a focus on the eastern U.S. coastal region or WNAO.

32 **Aerosol surface concentrations.** For comparison with model SNA surface concentrations, we use the
33 IMPROVE/CSN observations obtained at 59 eastern U.S. sites (in the states of NY, CT, VA, MA, ME, GA, PA, DC,
34 FL, NC, and SC), which are located upwind of the ACTIVATE flight area. **Fig. S1** shows the scatterplots of
35 IMPROVE/CSN daily surface concentrations of SNA aerosols versus corresponding model results at each of the
36 selected sites for Feb.-Mar. (upper panels) and Aug.-Sep. (lower panels), respectively, 2020. The model results from
37 both “standard” (blue triangles and lines) and “fixedCWC” (red triangles and lines) experiments (also see **Table 1**)
38 are shown to help understand the impact of using MERRA-2 CWC on simulated aerosols in GEOS-Chem. Model
39 daily output was sampled at the day, location, and site elevation for each data sample. In Feb.-Mar., for sulfate the
40 standard model with MERRA-2 CWC has a small overall bias (0.6%) relative to the observations, with a reduced-
41 major-axis (RMA) regression slope of 0.80 and a correlation coefficient (R) value of 0.46. The fixedCWC simulation

42 yields a better regression slope (0.98) but a much larger overall bias. The standard model overestimates nitrate and
43 ammonium substantially with an average positive bias of 198.5% and 230.3%, respectively. These biases in fixedCWC
44 are even higher. Using MERRA-2 CWC in the stratiform precipitation scavenging in the standard model is expected
45 to reduce existing large positive biases in surface nitrate and ammonium concentrations as demonstrated by Luo et al.
46 (2019, 2020). Our results here also show that using spatiotemporally varying CWC from MERRA-2 slightly expedites
47 aerosol scavenging and thus improves simulated aerosol concentrations. The improvement in our analysis is, however,
48 very limited. In Aug.-Sep., the standard model largely overestimates surface concentrations of sulfate (61.2% bias),
49 nitrate (97.4% bias), and ammonium (249.9% bias). Using MERRA-2 CWC has slightly reduced the model bias in
50 surface sulfate concentrations but increased the model biases in surface nitrate and ammonium concentrations. The
51 latter is inconsistent with Luo et al. (2020) probably due to not having fully implemented their modifications to sulfate
52 scavenging, which affects nitrate and ammonium through the SNA aerosol chemical dynamics. This also suggests that
53 the impact of individual modifications to SNA wet scavenging should be investigated separately because feedback
54 from complicated chemical dynamics is always involved.

55 **Aerosol wet deposition fluxes.** For comparison with model SNA wet deposition fluxes, we use the NADP
56 observations obtained at over 100 eastern U.S. sites (in the same states as for surface aerosol concentrations above).
57 **Fig. S2** shows the scatterplots of model monthly mean wet deposition fluxes of sulfate + SO₂, nitrate + nitric acid
58 (HNO₃), and ammonium + ammonia (NH₃) versus those from NADP for Feb.-Mar. and Aug.-Sep. 2020. The observed
59 sulfur deposition fluxes are mostly < 1.0 kg per ha per 30 days and did not change significantly from winter to summer.
60 In both seasons, the standard model with MERRA-2 CWC overestimates sulfate wet deposition fluxes (~57.9% bias
61 in winter and ~44.2% bias in summer), while the fixedCWC simulation results in reduced biases (~18.4% in winter
62 and 31.8% in summer). Correlation between either of the two simulations and observations is not strong (R<0.5),
63 suggesting that further improvement is required for sulfate scavenging. Observed wet deposition fluxes of nitrate tend
64 to decrease from winter to summer, presumably because of lower concentrations in summer (**Fig. S1**). In the
65 wintertime, both the standard and fixedCWC simulations overestimate nitrate deposition fluxes. The fact that model
66 simulations show large positive biases in both surface concentrations and deposition fluxes suggests that there is too
67 much nitrate mass in the model and/or nitrate is scavenged too fast at higher altitudes followed by partial release into
68 the air due to rainwater evaporation close to the surface. Compared to the fixedCWC simulation, the standard
69 simulation shows larger nitrate deposition flux overestimates due to faster scavenging with MERRA-2 CWC (Luo et
70 al., 2019). The observed ammonium wet deposition fluxes exhibit larger variability among all sites in summer relative
71 to winter. The fixedCWC simulation tends to underestimate ammonium deposition fluxes and shows values of similar
72 magnitude in the two seasons. The standard simulation with MERRA-2 CWC overcorrects this underestimate in winter
73 due to enhanced stratiform precipitation scavenging of ammonium, resulting in an overall positive bias of 46.1%. Such
74 effects are not seen for summertime ammonium likely because of the increased role of convective scavenging in
75 summer.

76 **MODIS AOD.** We compare model simulated AOD with MODIS observations with respect to the spatial
77 distribution of monthly mean AODs along with speciated AODs suggested by the model. **Fig. S3** shows model
78 monthly mean AODs in comparison with MODIS/Aqua retrievals (at 550 nm) over North America and the North

79 Atlantic for the months of Feb. and Mar., respectively, 2020. Model output is sampled daily at 1:30 pm local time
80 along the Aqua satellite orbit track. Also shown are contributions to the total AOD in the model from accumulation
81 mode sea salt (SSa), coarse mode sea salt (SSc), SNA, BC, organic carbon (OC), and dust. Model AODs in the
82 simulation “fixedCWC” (**Table 1**) are shown in the bottom panels. In general, the model underestimates AODs over
83 the WNAO during Feb.-Mar. 2020, with improved model performances along the south/east U.S. coast in March. The
84 former is likely ascribed to underestimated sea salt emissions because of MERRA-2’s tendency to underestimate ocean
85 surface winds (Carvalho, 2019) and coarse model grid resolution (Weng et al., 2020). The spatial variation of MODIS
86 AOD from the Midwest U.S. to the WNAO shows different patterns between Feb. and Mar. In Feb., MODIS observed
87 high AODs over the Midwest U.S., a decreasing trend towards the South/East U.S. Coast, and high AODs over the
88 WNAO. The model captures this spatial pattern but the magnitude of AOD variations is much smaller than observed
89 by MODIS. The spatial distribution of model simulated speciated AODs (**Fig. S3**) suggest that SNA aerosols over the
90 Midwest U.S. and coarse-mode sea salt over the WNAO are mainly responsible for this pattern in Feb. In Mar., MODIS
91 observed higher AODs in South/East U.S. Coast and over the WNAO compared to Feb. Such increases are also
92 captured by the model, which attributes the higher AODs to substantially increased OC and, to a lesser extent, more
93 SNA over the Midwest U.S. and coarse-mode sea salt over the WNAO. The low bias in AOD over the western U.S.
94 in the model is likely due to missing anthropogenic or BB emissions for the region, as the “fixedCWC” simulation
95 with slower wet scavenging does not remove this model bias. The latter simulation does yield higher AODs over the
96 WNAO, closer to the MODIS values. However, this could be a result of compensating effects between inefficient
97 aerosol wet scavenging and low sea salt emissions over the ocean. Model simulated AODs over the WNAO are
98 dominated by coarse-mode sea salt, SNA, OC, and accumulation-mode sea salt, with negligible contributions from
99 BC and dust.

100 **Fig. S4** shows the same plots as **Fig. S3**, but for the months of Aug. and Sep., respectively, 2020. In Aug., MODIS
101 observed much higher AODs over the western, southwestern, southeastern U.S., and WNAO, relative to the winter
102 months. The model reproduces the general spatial distribution but again underestimates AODs over the remote Atlantic
103 Ocean. The distribution of model speciated AODs suggests that OC explains most of the AOD spatial variation while
104 SNA also makes an important contribution. In September, MODIS observed even higher AODs over the western U.S.
105 coast (> 0.5), Midwest U.S., and WNAO. The model captures this month-to-month change in AODs very well and
106 attributes it to large increases in OC as well as coarse-mode sea salt aerosols. As expected, SNA AOD decreases from
107 Aug. to Sep., reflecting the seasonal reduction in secondary production of SNA aerosols. In summer 2020, extensive
108 wildfires occurred in the western and southeastern U.S. (section 5.4). In particular, the August Complex “Gigafire” in
109 mid-August 2020 and the California Creek fire in early September 2020 are among the most intensive fire events in
110 California. Primary organic aerosols and SOA from oxidation of VOCs emitted by these fires cause substantial
111 increases in AOD over both the fire emission source region and along the smoke transport pathway towards the
112 Midwest, northeast U.S., and WNAO, as observed by MODIS and simulated by the model. The generally much higher
113 AODs in summer relative to winter are mainly due to the much larger contributions from these smoke organic aerosols.
114 The model AOD low bias over the WNAO in Aug. appears to be at least partly due to underestimate of sea salt
115 emissions, which are lower than those for Feb., Mar., and Sep. In addition, BC from the wildfires makes non-negligible

116 contributions to summertime AOD over the western and Midwest U.S., in contrast to the wintertime. Model dust AOD
117 distributions indicate transport of dust from tropical eastern Atlantic and North Africa to the WNAO region during the
118 summer months, especially Aug. 2020, in agreement with MODIS AOD observations. Using MERRA-2 CWC for
119 stratiform precipitation scavenging of aerosol in the standard model has little effects on model simulated AOD in
120 Aug.-Sep., when compared to those from the “fixedCWC” simulation (bottom panels, **Fig. S4**). This is due to the
121 dominant role of convective (versus stratiform) precipitation in scavenging aerosols during summer.

122

123 **References**

124

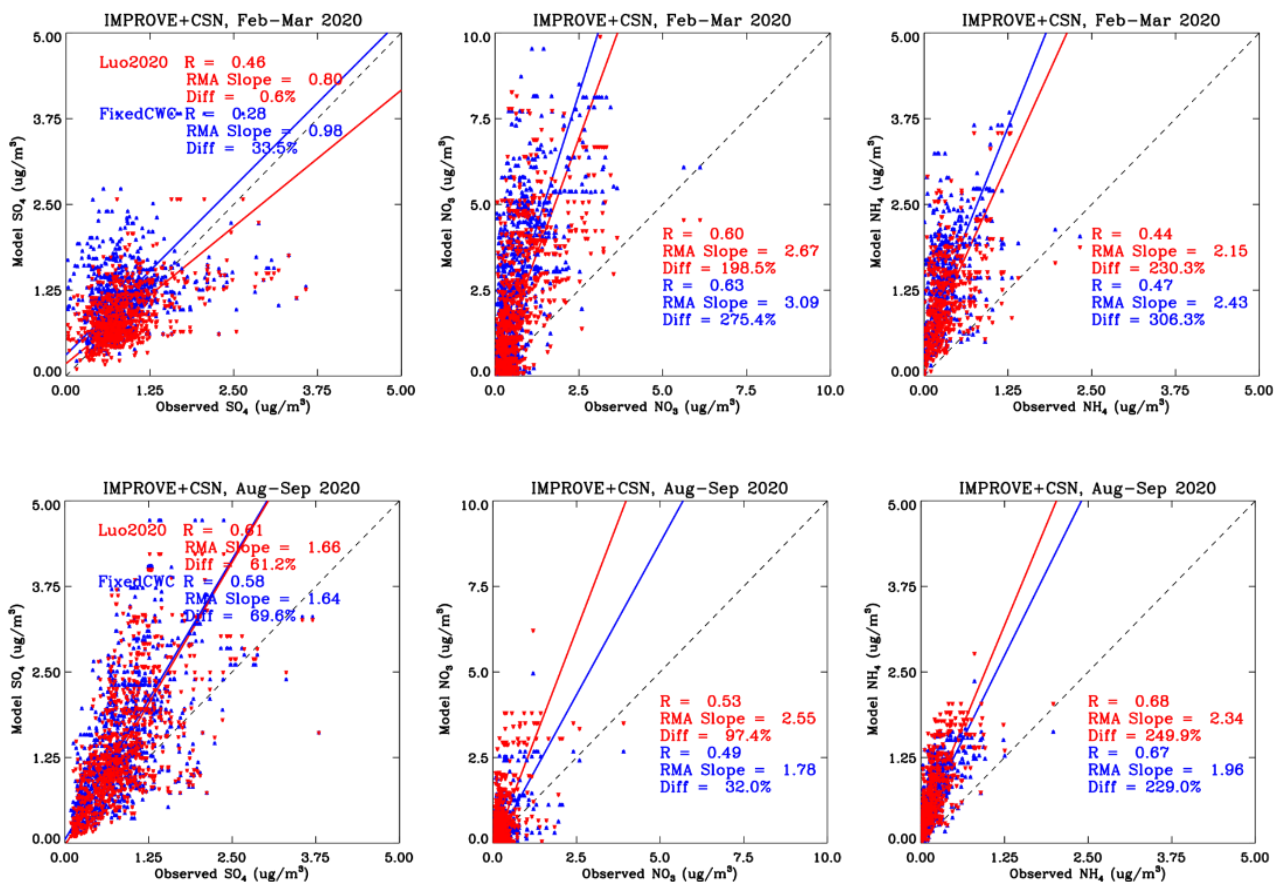
125 Carvalho, D.: An Assessment of NASA’s GMAO MERRA-2 Reanalysis Surface Winds, *J. Climate*, 32(23), 8261–
126 8281, doi:10.1175/JCLI-D-19-0199.1, 2019.

127 Philip, S, Marin, R. V., Pierce, J. R., Jimenez, J. L., Zhang, Q., Canagaratna, M. R., Spracklen, D. V., Nowlan, C. R.,
128 Lamsal, L. N., Cooper, M. J., and Krotkov, N. A., Spatially and seasonally resolved estimate of the ratio of organic
129 mass to organic carbon, *Atmos. Environ.*, 87, 34-40, <http://dx.doi.org/10.1016/j.atmosenv.2013.11.065>, 2014.

130 Weng, H.-J., Lin, J.-T. *, Martin, R., Millet, D. B., Jaeglé, L., Ridley, D., Keller, C., Li, C., Du, M.-X., and Meng, J.,
131 Global high-resolution emissions of soil NO_x, sea salt aerosols, and biogenic volatile organic compounds,
132 *Scientific Data*, 7, 148, doi:10.1038/s41597-020-0488-5, 2020.

133

134
135
136



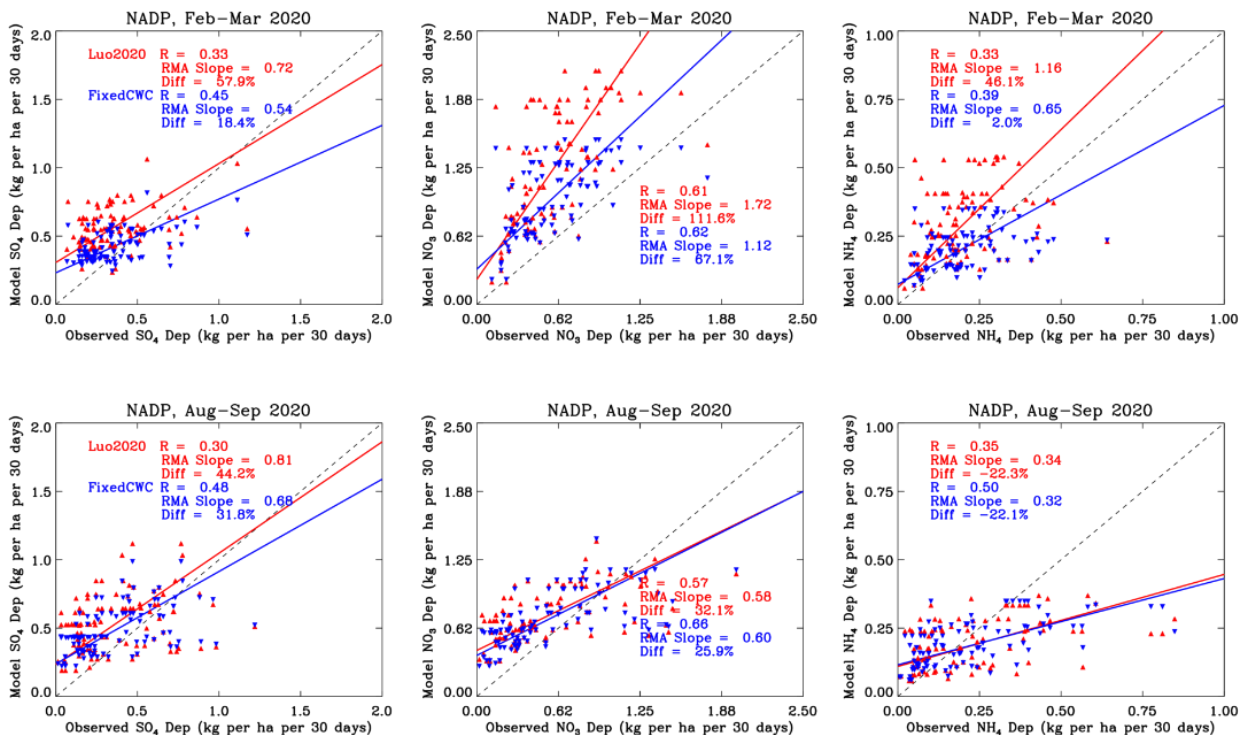
137

138

139 **Figure S1.** Scatterplots of model daily mean surface concentrations of SO₄, NO₃, and NH₄ versus corresponding IMPROVE and
140 CSN observations made at near-coast eastern U.S. sites during Feb.-Mar. (upper panels) and Aug.-Sep. (lower panels) 2020,
141 respectively. Model results from simulations with either a fixed cloud water content (blue; Table 1) or MERRA-2 cloud water
142 content (red; Table 1) are shown. Solid lines are the linear regression lines obtained using the reduced-major-axis (RMA)
143 method. Dashed lines are 1:1 line. Legends show calculated correlation coefficient, RMA slope (if R > 0.1), and overall difference (%)
144 between model results and observations, i.e., $(\sum \text{model} - \sum \text{observation}) / \sum \text{observation} \times 100\%$.

145

146
147
148



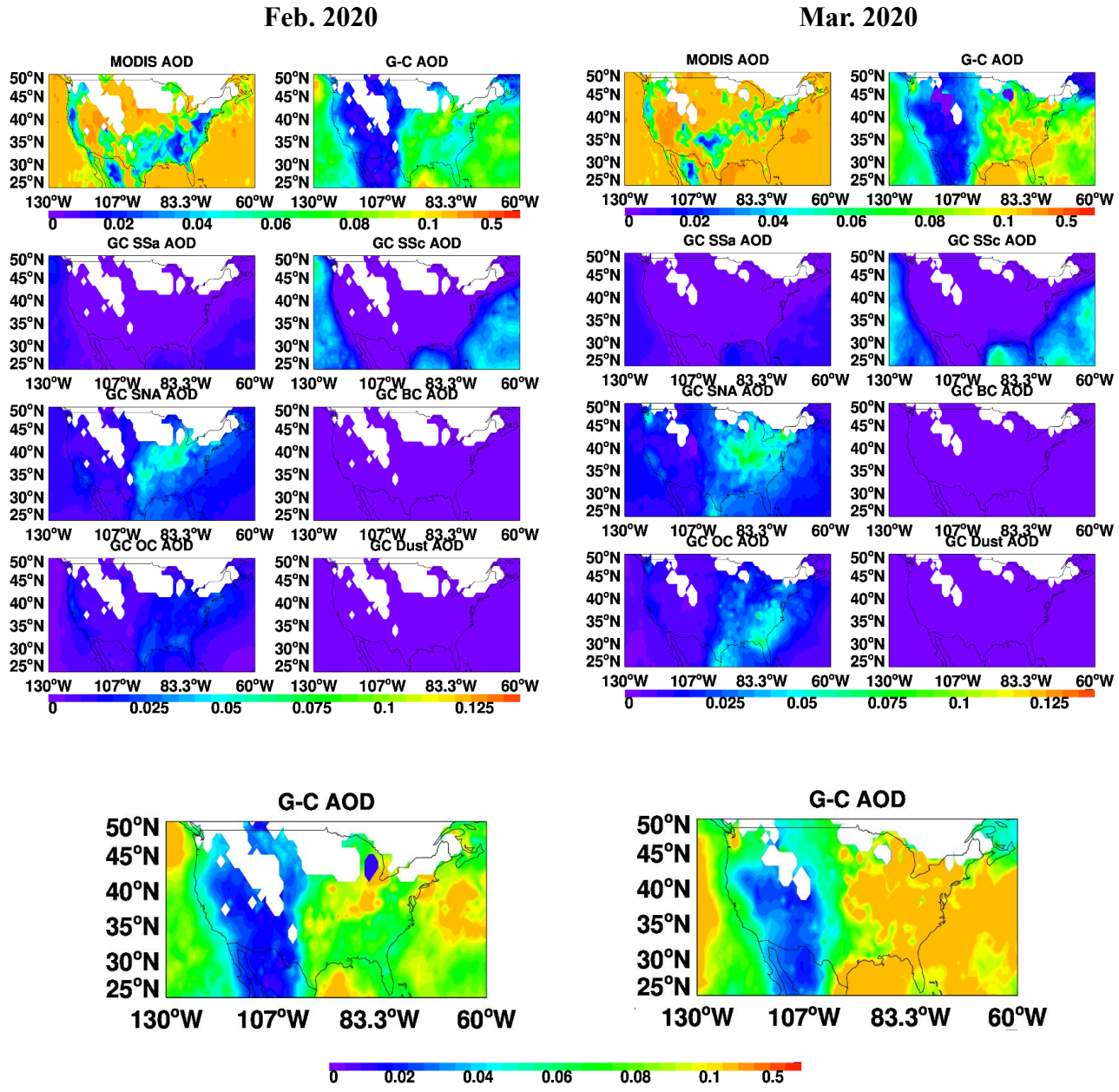
149

150

151 **Figure S2.** Scatterplots of model monthly mean wet deposition fluxes of SO₄+SO₂, NO₃+HNO₃, and NH₄+NH₃ versus
152 corresponding NADP observations made at near-coast eastern U.S. sites (>100 sites in the states of NY, CT, VA, MA, ME, GA,
153 PA, DC, FL, NC, and SC) during Feb.-Mar. (upper panels) and Aug.-Sep. (lower panels) 2020, respectively. Deposition mass fluxes
154 of SO₂, HNO₃, and NH₃ are converted to SO₄, NO₃, and NH₃ mass fluxes of equivalent mole amounts. Monthly mean model results
155 are sampled at the month and location of observations. Each data point in the figure represents a monthly mean value for one single
156 site. Model results from simulations with either a fixed cloud water content (blue; Table 1) or MERRA-2 cloud water content (red;
157 Table 1) are shown. Solid lines are the linear regression lines obtained using the reduced-major-axis (RMA) method. Dashed lines
158 are 1:1 line. Legends show calculated correlation coefficient, RMA slope (if R > 0.1), and overall difference (%) between model
159 results and observations: $(\sum_{model} - \sum_{observation}) / \sum_{observation} \times 100\%$.

160

161
 162
 163
 164
 165
 166
 167
 168
 169
 170
 171
 172
 173
 174
 175
 176
 177
 178
 179
 180
 181
 182
 183
 184
 185



186 **Figure S3.** Evaluation of model monthly mean AODs with MODIS/Aqua retrievals (at 550nm) over North America and North
 187 Atlantic for Feb. 2020 (left two columns) and Mar. 2020 (right two columns). Model output is sampled daily at 1:30 pm local time
 188 along the Aqua satellite orbit track. Also shown are contributions to the total AOD in the model from accumulation mode sea salt
 189 (SSa), coarse mode sea salt (SSc), sulfate-nitrate-ammonium (SNA), black carbon (BC), organic carbon (OC, primary only), and
 190 dust. Model AODs in the simulation “fixedCWC” (Table 1) are shown in the bottom panels.

191

192
 193
 194
 195
 196
 197
 198
 199
 200
 201
 202
 203
 204
 205
 206
 207
 208
 209
 210
 211
 212
 213
 214
 215
 216
 217
 218

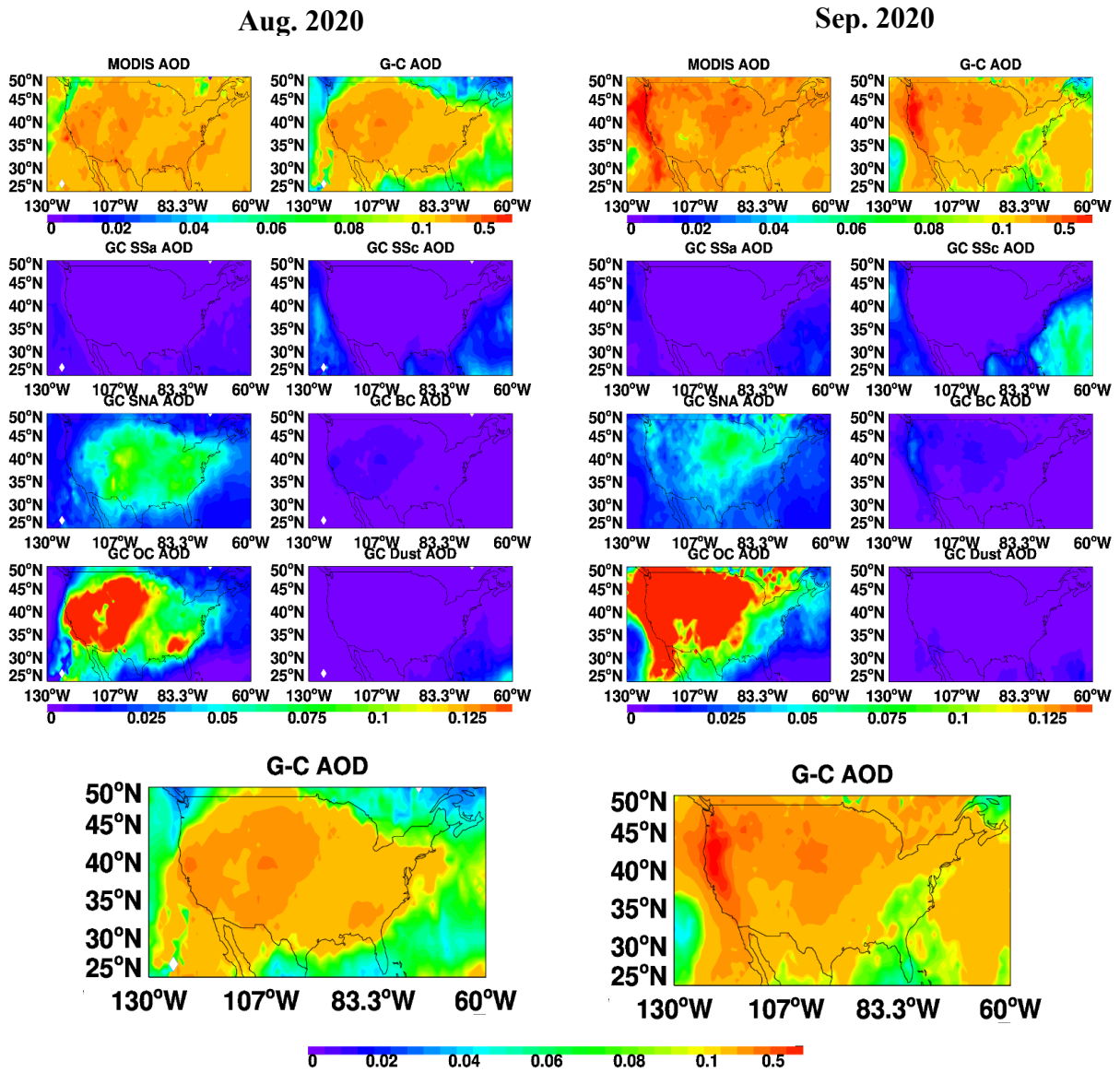


Figure S4. Same as Fig. S3, but for Aug. 2020 (left two columns) and Sep. 2020 (right two columns).

219
220
221
222
223
224
225
226
227
228
229
230
231
232
233
234
235
236

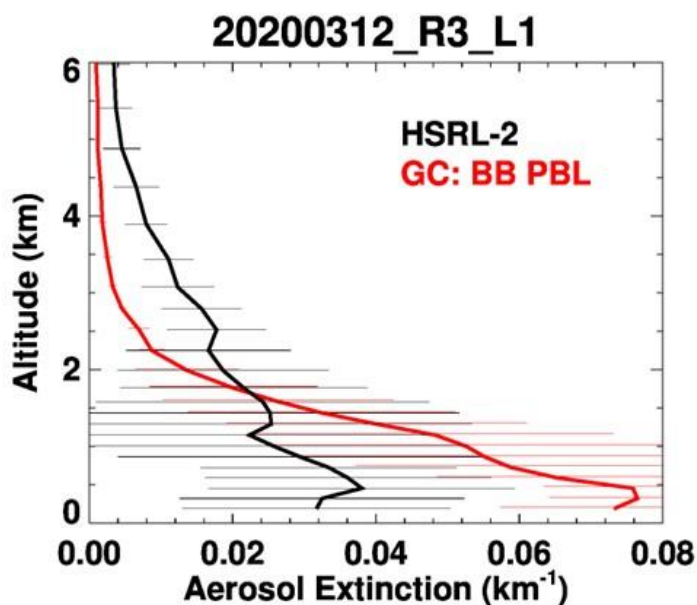
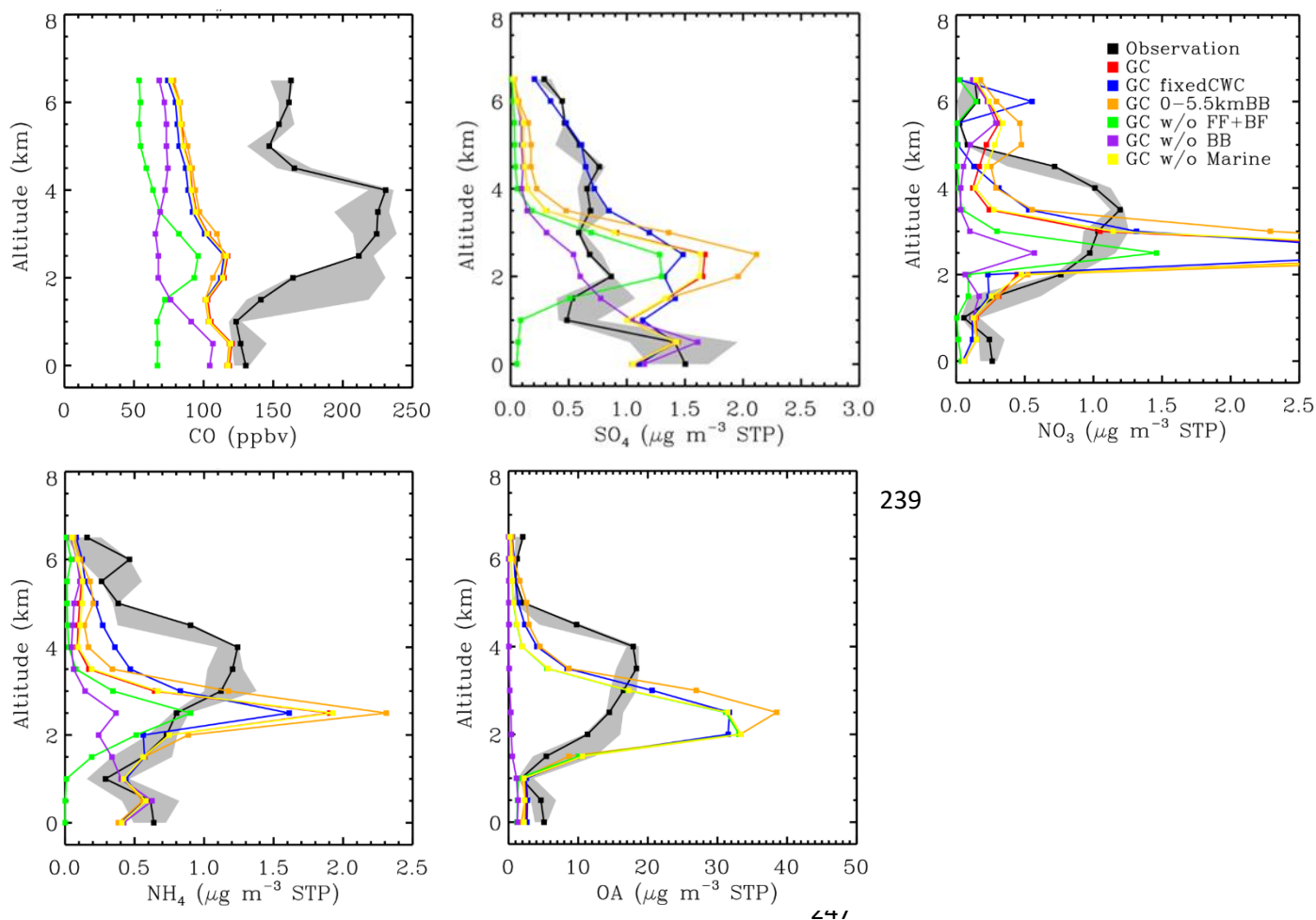


Figure S5. Comparisons of model aerosol extinctions (550nm) with aircraft HSRL-2 lidar measurements (532nm) averaged over the morning flight on March 12, 2020. Biomass burning emissions are injected into the planetary boundary layer (“BB PBL”) in the model (see Table 1). Hourly model output was sampled at the time and location of lidar measurements. Horizontal lines denote +/- standard deviations of observed and simulated aerosol extinctions at model vertical levels.

237

238



239

248

249 **Figure S6.** Comparison of model simulated (red) vertical profiles of CO (ppbv), sulfate, nitrate, ammonium, and organic aerosol
250 (OA; $\mu\text{g m}^{-3}$ STP) mixing ratios with Falcon aircraft measurements (black) on Sep. 23, 2020. Also shown are model results from
251 simulations (Table 1) with (1) a fixed value for cloud water content used in aerosol scavenging (“fixedCWC”), (2) biomass burning
252 emissions injected to the 0-5.5km altitudes, (3) fossil fuel and biofuel emissions turned off, (4) biomass burning emissions turned
253 off, or (5) marine emissions turned off, respectively. An OA/OC ratio of 2.1 (Philip et al., 2014) is used to convert simulated OC
254 to compare with AMS OA measurements. Hourly model output was sampled at the time and location of aircraft measurements.
255 Values (500m-binned) are medians. Gray shaded areas indicate the ranges of 25th – 75th percentiles for the observations.

256